



# STRUCTURAL MOBILITIES FOR THE EDGE-EXCITED, SEMI-INFINITE CYLINDRICAL SHELL USING A PERTURBATION METHOD

O. FÉGEANT

*Department of Building Sciences, Royal Institute of Technology (KTH), SE-100 44 Stockholm, Sweden.*

*E-mail: [Olivier@bim.kth.se](mailto:Olivier@bim.kth.se)*

*(Received 30 November 2000, and in final form 1 May 2001)*

In this paper, the problem of the vibrational response of a thin-walled cylindrical, semi-infinite shell subject to edge loads is addressed. The loads consist of an axial force, a circumferential force, a radial force and a bending moment. Approximate solutions for input mobilities as well as cross-mobilities associated with the loads are obtained in closed form using the method of the matched asymptotic expansions. The accuracy of the expressions derived is discussed by comparing the approximate results obtained both for mobilities for a given circumferential mode of vibration and point mobilities to numerical results calculated using Flügge theory. It is shown that vibrational power transmission by mechanical point excitation is predicted with an acceptable level of agreement for a frequency below half the ring frequency.

© 2001 Academic Press

## 1. INTRODUCTION

In a noise and vibration control context, it is important to understand and quantify the vibration transmission to cylindrical shells by dynamical excitations such as forces and moments. To this end a most convenient concept is structural mobility, because of the simple relationship existing between the input power into an elastic structure and the real part of its mobilities. However, in the case of cylindrical shells, the mobility representation is considerably complicated by the coupling occurring between in-plane and out-of-plane vibrations. Indeed, cross-mobility, or the complex ratio of velocity in one direction to force or moment in another direction, can play a decisive role in the vibration transmission to shells, such as in the case of joint excitation.

By virtue of the cylindrical symmetry of the shell, loads applied and displacement produced can be expanded in a sum of modes by means of Fourier series expansions in the circumferential direction. The structural mobilities of the shell can then be calculated for each mode in a relatively simple way. Furthermore, owing to the waveguide character of shells, only a finite number of circumferential modes are able to propagate freely at a given frequency, that is contributes to the vibrational power transmission. This waveguide behaviour simplifies the analysis of vibration transmission substantially [1], as only the modes that are propagating are needed for the calculation of the input mechanical power.

The mobilities of the cylindrical shell of infinite extent are of considerable interest in particular [1–6], as they provide estimates of the mobilities for a similar but finite shell in a frequency-averaged sense. However, in practice shells are often subject to forces and moments located at their edges, thereby invalidating the aforementioned analogy and

motivating the investigation of the edge-excited, semi-infinite shell. The boundary-value problem of the semi-infinite shell being acted upon by edge loads was first addressed and solved explicitly in the static case by Simmonds in 1966 [7]. With regard to dynamical excitation, both problem formulation and computed results for the input and cross-mobilities were presented recently by Ming *et al.* [8], while closed-form solutions for both the infinite and semi-infinite shell problems under axially symmetrical loads have been derived by the author in a previous article [9].

The main focus of this paper is the derivation of approximate solutions for the input and cross-mobilities of the semi-infinite, cylindrical shell excited at its edge by forces and moments with other circumferential distributions. The study is confined to *in vacuo* vibrations, and the shell is assumed to be sufficiently thin to satisfy Love's first approximations. Four load types are considered in relation to the excitation: an axial force, a circumferential force, a radial force and a bending moment. The size of the region of excitation in the axial direction is assumed to be larger than the shell thickness, but relatively small compared to the axial wavelength. The edge loads are assumed to have slow spatial variations in the circumferential direction and exerted at a frequency below the ring frequency of the shell (that is the frequency at which the wavelength of extensional waves in the shell wall coincides with the shell circumference). Consequently, only the modes of low-circumferential order ( $n = 0, 1, 2, 3 \dots$ ) are excited. The underlying reason for these restrictions is two-fold. Firstly, a high proportion of the noise and vibration problems in which shells are involved, arise at frequencies below the ring frequency. Secondly, the analysis is thus limited to these vibrations, which are characteristic of shells in the sense that only vibrations for which a strong coupling between radial, circumferential and axial motions occurs are studied. At higher frequency, or for modes of high-circumferential order, the vibrational behaviour of the shell tends to liken that of the plate strip and can thus be studied through the in-plane and out-of-plane governing equations for thin plates [10, 11].

Well below the ring frequency, membrane theory [2, 12] is often used as a simplified shell theory to model the shell vibrations. This is especially so for the axisymmetric mode ( $n = 0$ ), the beam mode ( $n = 1$ ) and other lower modes excited to well above their cut-on frequencies. However, this theory alone cannot satisfy all the boundary conditions associated with the edge loads. Furthermore, it fails to model the cut-on phenomena experienced by the circumferential modes, which is largely responsible for the power input to the shells. In the analysis presented here, the boundary-value problem is handled by describing the shell vibrations and the boundary conditions by using the Donnell–Mushtari shell equations, where tangential inertial forces are neglected. Perturbation solutions are then sought by applying the method of the matched asymptotic expansions [9, 13]. According to this method, the shell is modelled as a membrane at some distance from the edge but bending actions localized in the edge region can also be accounted for. In this regard, the method distinguishes between an inner region adjoining the edge and an outer region describing the main body of the shell. Simplified but different sets of governing equations are derived for both regions, which can be solved analytically in the case presented. Solutions are obtained in the form of power-series expansions for which the expansion parameter is a function of the shell thickness-to-radius ratio multiplied by the circumferential modal order  $n$ . Thus, the solutions of the inner region satisfy the boundary conditions associated with the present boundary-value problem, while in the outer region, the solutions are to some extent, solutions to the membrane shell equations. Furthermore, matching the inner solution to the outer one provides additional conditions, which lead to the complete determination of these solutions. The leading terms of these expansions then yield approximate expressions for the elements of the mobility matrix. Finally, the expressions derived are corrected to account partly for the influence of the inertial force of

the circumferential displacement, and compared with the results obtained using Flügge shell theory for the mobilities of both the individual modes and point excitations.

2. FORMULATION OF THE BOUNDARY-VALUE PROBLEM

Consider the circular, semi-infinite shell of mean radius  $R$  and thickness  $h$  sketched in Figure 1. The shell is assumed to be thin, made of homogeneous isotropic material and acted upon by a set of edge loads specified by the following set of equations:

$$\begin{aligned} N_s &= N_n \cos(n\phi)e^{i\omega t}, & T_s &= T_n \sin(n\phi)e^{i\omega t}, \\ R_s &= R_n \cos(n\phi)e^{i\omega t}, & M_s &= M_n \cos(n\phi)e^{i\omega t}, \end{aligned} \tag{1}$$

where the integer  $n$  is the circumferential modal number,  $\omega$  the circular frequency of the excitation, and  $t$  the time. In this paper, it is assumed that  $n > 0$  since the mode  $n = 0$  has been treated in detail elsewhere [9].  $N_s, T_s, R_s$  are force components in the axial, tangential and radial directions, respectively, while  $M_s$  is a bending moment. The loads refer to a unit length of section and are defined positive accordingly to Figure 1. It is worth noting that excitation by a twisting moment does not need to be considered, as such a load type can be replaced by statically equivalent distributions of  $T_s$  and  $R_s$  [14].

Let us assume first that the vibration field produced in the shell body is predominantly radial, thereby allowing us to neglect in-plane inertial forces in the shell equations of motion. The vibrations of the shell in vacuum are then conveniently expressed in terms of a function  $\Phi$  [15], obeying the eighth order differential equation,

$$\beta \nabla^8 \Phi + (1 - \mu^2) \Phi'''' + \frac{\rho(1 - \mu^2)R^2}{E} \nabla^4 \ddot{\Phi} = 0, \tag{2}$$

where

$$s = \frac{x}{R}, \quad (') = \frac{\partial(\ )}{\partial s}, \quad (')^\bullet = \frac{\partial(\ )}{\partial \phi}, \quad (\dot{\ }) = \frac{\partial(\ )}{\partial t}, \quad \nabla^2(\ ) = (')'' + (')^{\bullet\bullet} \quad \text{and} \quad \beta = \frac{h^2}{12R^2}.$$

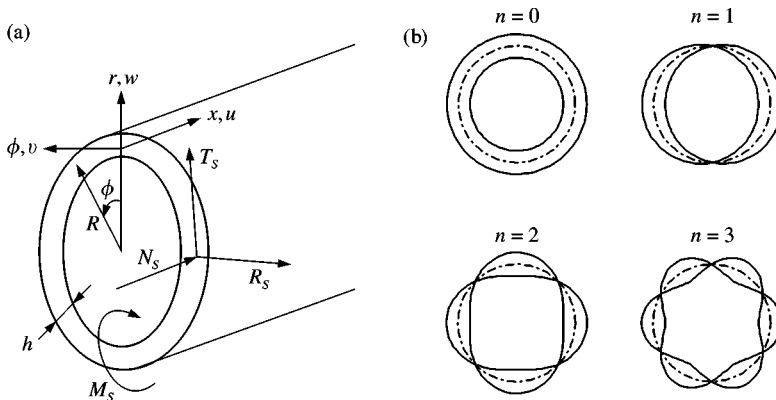


Figure 1. The semi-infinite shell: (a) co-ordinate system and positive convention of force and moment; (b) modal shape of the circumferential modes  $n = 0, 1, 2$  and  $3$ .

The parameters  $\mu$ ,  $\rho$  and  $E$  are the Poisson ratio, the density and the Young's modulus of the shell material, respectively, and  $\beta$  is referred to as the thickness parameter of the shell.

The shell displacements in the axial ( $u$ ), circumferential ( $v$ ) and radial directions ( $w$ ) are related to  $\Phi$  by the equations

$$u = \Phi'' - \mu\Phi''', \quad v = -\Phi''' - (2 + \mu)\Phi'' \quad \text{and} \quad w = \nabla^4 \Phi. \tag{3}$$

Considering the semi-infinite shell where  $0 < s < \infty$ , the general form of solutions to equation (2) is

$$\Phi(s, \phi, t) = \Phi_n \cos(n\phi) e^{i\omega t}, \tag{4}$$

where

$$\Phi_n = C_1 e^{\kappa_1 s} + C_2 e^{\kappa_2 s} + C_3 e^{\kappa_3 s} + C_4 e^{\kappa_4 s}. \tag{5}$$

The propagation constants  $\kappa_j$  are the roots of the dispersion relation associated with equation (2), which are located in the complex half-plane  $\pi/2 < \arg(\kappa) \leq 3\pi/2$ . The wave amplitudes  $C_j$  are obtained from the boundary conditions. The boundary conditions for the boundary-value problem under consideration here (where the forces and moments are prescribed at the edge) are derived by inserting the function  $\Phi$  into the stress resultants obtained with the Donnell–Mushtari theory [16] as follows:

$$\begin{aligned} N_n &= \frac{B}{R} n^2 (1 - \mu^2) \Phi_n''|_{s=0}, \\ T_n &= -\frac{1 - \mu^2}{R} nB (\Phi_n''' + \frac{\beta}{1 + \mu} \nabla^4 \Phi_n')|_{s=0}, \\ R_n &= \frac{D}{R^3} \nabla^4 (\Phi_n''' - (2 - \mu)n^2 \Phi_n')|_{s=0} \quad \text{and} \\ M_n &= -\frac{D}{R^2} \nabla^4 (\Phi_n'' - \mu n^2 \Phi_n)|_{s=0}, \end{aligned} \tag{6}$$

where

$$B = \frac{Eh}{1 - \mu^2} \quad \text{and} \quad D = \frac{Eh^3}{12(1 - \mu^2)}.$$

Once equation (5) is introduced into boundary conditions (6) and the system solved for  $C_j$ , the shell velocities, and consequently the shell mobilities, may readily be obtained by using equations (3).

Presented in matrix form, the shell mobilities read explicitly as

$$\begin{bmatrix} \dot{u}_n \\ \dot{v}_n \\ \dot{w}_n \\ \dot{\theta}_n \end{bmatrix} = \begin{bmatrix} Y_{uN}^n & Y_{uT}^n & Y_{uR}^n & Y_{uM}^n \\ Y_{vN}^n & Y_{vT}^n & Y_{vR}^n & Y_{vM}^n \\ Y_{wN}^n & Y_{wT}^n & Y_{wR}^n & Y_{wM}^n \\ Y_{\theta N}^n & Y_{\theta T}^n & Y_{\theta R}^n & Y_{\theta M}^n \end{bmatrix} \begin{bmatrix} N_n \\ T_n \\ R_n \\ M_n \end{bmatrix}, \tag{7}$$

where  $\theta$  represents the rotation of the normal to the middle surface about the  $\phi$ -axis,  $\theta = \partial w / \partial x$ . The mobility matrix is symmetrical and its diagonal and off-diagonal coefficients are referred to as input and cross-mobilities respectively. They are obtained from the constants  $C_j$  by using the equations

$$\begin{aligned}
 Y_{uX}^n &= -i\omega \sum_{j=1}^4 \kappa_j (\mu \kappa_j^2 + n^2) C_j, & Y_{vX}^n &= i\omega \sum_{j=1}^4 n((2 + \mu)\kappa_j^2 - n^2) C_j, \\
 Y_{wX}^n &= i\omega \sum_{j=1}^4 (\kappa_j^2 - n^2)^2 C_j, & Y_{\theta X}^n &= \frac{i\omega}{R} \sum_{j=1}^4 (\kappa_j^2 - n^2)^2 \kappa_j C_j,
 \end{aligned}
 \tag{8}$$

where  $X$  denotes one of the excitation components (either  $N_n$ ,  $T_n$ ,  $R_n$  or  $M_n$ ). For the determination of the mobilities relative to  $X$ , the wave amplitudes  $C_j$  are calculated by assuming that  $X$  equals one and the other components equal zero.

Despite the rather simple formulation of the boundary-value problem being considered, closed-form solutions for the coefficients of the mobility matrix are precluded due to the cumbersome analytical expressions of the propagation constants. Accordingly, approximate solutions are sought by using perturbation techniques. With this in mind, equation (2) is re-written with a variable change  $\bar{s} = ns$ , yielding

$$\beta n^4 (\Phi_n'''''' - 4\Phi_n'''' + 5\Phi_n'''' - 2\Phi_n'') + 4m^4 \Phi_n'''' + 2\sigma^2 \Phi_n'' - \sigma^2 \Phi_n = 0,
 \tag{9}$$

where primes now denote differentiation with respect to  $\bar{s}$ , and where the notation

$$\Omega^2 = \frac{\rho(1 - \mu^2)\omega^2 R^2}{E}, \quad \sigma^2 = \Omega^2 - \beta n^4, \quad 4m^4 = 1 - \mu^2 - \sigma^2
 \tag{10}$$

has also been introduced.

### 3. THE PERTURBATION METHOD

In differential equation (2), the highest derivative is multiplied by the parameter  $\beta n^4$ . Provided that  $\beta n^4 \ll 1$  (which means that the shell vibrates in one of its lower circumferential modes) the boundary-value problem is seen as belonging to the class of the *edge-layer* problems [17]. In the case under consideration, it is translated into axial variations of the shell motions characterized by two distinct length scales. One scale is associated with motions remaining localized in the edge region, while the other scale is characteristic of motions penetrating farther into the shell body. This class of problems lends itself to analysis by perturbation techniques and particularly by the method of matched asymptotic expansions.

As mentioned in the introduction, this method divides the body of the shell into an inner region adjoining the edge and an outer region including the rest of the structure. In the inner region, the governing equation and the boundary conditions are re-arranged using a magnified scale and expanded as a function of the parameter  $\beta^{1/4}n$ . The solution to these equations is referred to as the inner solution. In the outer region, the equation of motion is expanded by using the original co-ordinate system and the associated solution is termed the outer solution. The basic idea underlying the method is that the domains of validity for the two expansions overlap. This matching provides the additional equations that allow all of the constants in the expansions to be determined. Finally, combining the inner and outer

expansions forms a composite expansion that is valid for both the inner and the outer regions.

### 3.1. THE INNER PROBLEM

In the inner region, a stretched co-ordinate system is used, reading  $\zeta = \bar{s}/(\beta n^4)^\varepsilon$  in its general form. The parameter  $\varepsilon$  is a strictly positive constant and has to be determined. This is achieved by searching for the value of  $\varepsilon$  that yields the least degenerate limit of differential equation (2) when  $\beta n^4 \rightarrow 0$  in the new co-ordinate system [17]. It ensues here that  $\varepsilon = 1/4$  and thus the inner solution has to be sought in a power series in the form

$$\Phi^i = \sum_{k=0}^{\infty} \lambda^k \tilde{\Phi}_k, \tag{11}$$

where the expansion parameter  $\lambda$  is defined by

$$\lambda = \beta^{1/4} n. \tag{12}$$

The governing equations and boundary conditions satisfied by the functions  $\tilde{\Phi}_k$  (the successive terms of the expansion), are derived by inserting equation (11) into equations (2) and (6) expressed in the stretched co-ordinate system  $\zeta = \bar{s}/\lambda$ . Finally, terms of equal power of  $\lambda$  are collected. Upon adopting the convention  $\tilde{\Phi}_k = 0$  for  $k < 0$ , the governing equations (13) and boundary conditions (14) read

$$\tilde{\Phi}_k'''''' + 4m^4 \tilde{\Phi}_k'''' = 4\tilde{\Phi}_{k-2}'''' - 2\sigma^2 \tilde{\Phi}_{k-2}'' - 5\tilde{\Phi}_{k-4}'''' + \sigma^2 \tilde{\Phi}_{k-4} + 2\tilde{\Phi}_{k-6}'' \tag{13}$$

and

$$\begin{aligned} \tilde{N}_n \delta_{k2} &= \tilde{\Phi}_k'', \\ \tilde{T}_n \delta_{k3} &= \tilde{\Phi}_k'''' + (\tilde{\Phi}_{k-2}'''' - 2\tilde{\Phi}_{k-4}'''' + \tilde{\Phi}_{k-6}'') / ((1 + \mu)n^2), \\ \tilde{R}_n \delta_{k7} &= \tilde{\Phi}_k'''''' - (4 - \mu)\tilde{\Phi}_{k-2}'''' + (5 - 2\mu)\tilde{\Phi}_{k-4}'' - (2 - \mu)\tilde{\Phi}_{k-6}', \\ \tilde{M}_n \delta_{k6} &= \tilde{\Phi}_k'''''' - (2 + \mu)\tilde{\Phi}_{k-2}'''' + (1 + 2\mu)\tilde{\Phi}_{k-4}'' - \mu\tilde{\Phi}_{k-6} \end{aligned} \tag{14}$$

with the notation

$$\tilde{N}_n = \frac{R}{(1 - \mu^2)n^4 B} N_n, \quad \tilde{T}_n = -\frac{R}{(1 - \mu^2)n^4 B} T_n, \quad \tilde{R}_n = \frac{R^3}{Dn^7} R_n \quad \text{and} \quad \tilde{M}_n = -\frac{R^2}{Dn^6} M_n \tag{15}$$

and where  $\delta$  is the Kronecker delta function defined by

$$\delta_{km} = \begin{cases} 0 & \text{if } k \neq m, \\ 1 & \text{if } k = m. \end{cases}$$

3.2. THE OUTER PROBLEM

The outer solution is sought in a power series by using the form

$$\Phi^o = \sum_{k=0}^{\infty} \lambda^k \hat{\Phi}_k. \tag{16}$$

The differential equations governing the functions  $\hat{\Phi}_k$  are derived by inserting equation (16) into equation (2) and collecting terms of equal power of  $\lambda$ . Adopting the convention  $\hat{\Phi}_k = 0$  for  $k < 0$ , they read

$$4m^4 \hat{\Phi}_k'''' + 2\sigma^2 \hat{\Phi}_k'' - \sigma^2 \hat{\Phi}_k = -\hat{\Phi}_{k-4}'''''' + 4\hat{\Phi}_{k-4}'''' - 5\hat{\Phi}_{k-4}'' + 2\hat{\Phi}_{k-4}. \tag{17}$$

Upon assuming an excitation frequency well above the cut-on frequency for the investigated mode, that is  $\sigma^2 \cong \Omega^2$ , equation (17) reduces to the governing equation for membrane shells for the orders  $k = 0 \dots 3$ , when in-plane inertial forces are neglected.

3.3. THE MATCHING EQUATIONS

In the inner region, the general form of the solution to equation (13) is

$$\tilde{\Phi}_k = \sum_{p=0}^{\text{Int}(k/2)} (C_{k,p}^{(1)} \zeta^p e^{\rho_1 \zeta} + C_{k,p}^{(2)} \zeta^p e^{\rho_2 \zeta}) + \sum_{p=0}^{3 + 2\text{Int}(k/2)} C_{k,p}^{(3)} \zeta^p, \tag{18}$$

while in the outer region, the solution to equation (17) is

$$\hat{\Phi}_k = \sum_{p=0}^{\text{Int}(k/4)} (D_{k,p}^{(1)} \bar{s}^p e^{\kappa_1 \bar{s}} + D_{k,p}^{(2)} \bar{s}^p e^{\kappa_2 \bar{s}}), \tag{19}$$

where  $\text{Int}(x)$  denotes the integer part of  $x$ , and where the propagation constants are given by

$$\rho_1 = -m(1 + i), \quad \rho_2 = -m(1 - i), \quad \kappa_1 = -\sqrt{\frac{\sigma}{\sigma + \sqrt{1 - \mu^2}}}, \quad \kappa_2 = -\sqrt{\frac{\sigma}{\sigma - \sqrt{1 - \mu^2}}}. \tag{20}$$

The constants  $C_{k,0}^{(1)}$ ,  $C_{k,0}^{(2)}$ ,  $C_{k,p}^{(3)}$  and  $D_{k,0}^{(j)}$  describe the general solutions to equations (13) and (17) and have to be determined from both the boundary conditions and the matching equations. On the other hand, the constants  $C_{k,p}^{(1)}$ ,  $C_{k,p}^{(2)}$  and  $D_{k,p}^{(j)}$ , where  $p > 0$ , are associated with particular solutions appearing when these equations become non-homogeneous.

In accordance with the method presented in reference [17], the matching principle used to infer the matching equations is

$$\lim_{\bar{s} \rightarrow 0} \Phi^o(\bar{s}; \lambda) = \lim_{\zeta \rightarrow +\infty} \Phi^i(\zeta; \lambda). \tag{21}$$

Consider the case where the inner solution is given by equation (18). The polynomial part can be re-expressed in terms of the original variable  $\bar{s}$  while the exponential functions describing a standing decaying field are disregarded as  $\zeta \rightarrow \infty$ . The matching then being

performed as  $\bar{s} \rightarrow 0$  for the outer solution, equation (19) can be expanded in a Taylor series as follows:

$$\lim_{\bar{s} \rightarrow 0} \Phi^0(\bar{s}; \lambda) = \sum_{k=0}^{\infty} \lambda^k \sum_{j=0}^{\infty} \sum_{p=0}^{\text{Int}(k/4)} \frac{D_{k,p}^{(1)} \kappa_1^j + D_{k,p}^{(2)} \kappa_2^j}{j!} \bar{s}^{j+p}. \tag{22}$$

Matching is achieved by identifying the terms of the limits of the inner and outer solutions that are of equal power of  $\lambda$  and of  $\bar{s}$ . It can be shown that the two following conditions or matching equations ensue:

$$C_{k,m}^{(3)} = 0 \quad \forall k \quad \text{and} \quad \text{for } m > k \tag{23}$$

and

$$\sum_{p=0}^N \frac{D_{k,p}^{(1)} \kappa_1^{m-p} + D_{k,p}^{(2)} \kappa_2^{m-p}}{(m-p)!} - C_{k+m,m}^{(3)} = 0, \quad \forall m, \quad \forall k, \tag{24}$$

where  $N = \min(m, \text{Int}(k/4))$ .

### 3.4. THE COMPOSITE EXPANSION

Finally, the analysis is completed by deriving a composite solution that is valid in both the inner and the outer regions. According to Nayfeh [17], this composite expansion, denoted as  $\Phi^e$ , is defined by

$$\Phi^e = \Phi^0 + \Phi^i - \lim_{\bar{s} \rightarrow 0} \Phi^0(\bar{s}; \lambda). \tag{25}$$

Thus, upon using equations (11), (16), (18) and (19), plus the matching equations (23) and (24), the expression for the composite solution is

$$\Phi^e = \sum_{k=0}^{\infty} \lambda^k \left\{ \sum_{p=0}^{\text{Int}(k/4)} (D_{k,p}^{(1)} \bar{s}^p e^{\kappa_1 \bar{s}} + D_{k,p}^{(2)} \bar{s}^p e^{\kappa_2 \bar{s}}) + \sum_{p=0}^{\text{Int}(k/2)} (C_{k,p}^{(1)'} \bar{s}^p e^{\rho_1 \bar{s}} + C_{k,p}^{(2)'} \bar{s}^p e^{\rho_2 \bar{s}}) \right\}. \tag{26}$$

Terms in the form  $\bar{s}^p e^{\kappa \bar{s}}$  appear in the composite solution (26) as a consequence of the emergence of particular solutions. When  $\kappa$  describes a propagating wave, they become unbounded as  $\bar{s} \rightarrow \infty$  and thereby make the solution non-uniform. However, it has been shown that these terms are nothing but the power-series expansion of the propagation constants and consequently the non-uniformity can be removed by resorting once again to perturbation methods, such as the Lindstedt–Poincaré technique [19].

### 3.5. THE RADIAL EXCITATION CASE

The method is further exemplified here by looking at the case of radial excitation. As the other types of excitation can also be handled in a similar manner; only the final results are reported in the next section. Since it is assumed that the shell is acted upon by a radial force only,  $\tilde{N}_n$ ,  $\tilde{T}_n$  and  $\tilde{M}_n$  are all assigned a value of zero in boundary conditions (14) and the condition on the applied force has to be satisfied by the seventh order solution to the



inner region. Applying these boundary conditions and the matching equations (23) and (24), it can be shown that the inner solution to the seventh order is

$$\tilde{\Phi}_7 = C_{7,0}^{(1)}e^{\rho_1\zeta} + C_{7,0}^{(2)}e^{\rho_2\zeta} + \sum_{p=0}^3 C_{k,p}^{(3)}\zeta^p, \tag{27}$$

$$\begin{Bmatrix} C_{7,0}^{(1)} \\ C_{7,0}^{(2)} \end{Bmatrix} = \frac{1}{4m^4} \begin{Bmatrix} -1 \\ \frac{\rho_1^2(\rho_1 - \rho_2)}{1} \\ 1 \\ \frac{\rho_2^2(\rho_1 - \rho_2)}{\rho_1^2(\rho_1 - \rho_2)} \end{Bmatrix} \tilde{R}_n \quad \text{and} \quad \begin{Bmatrix} C_{6,2}^{(3)} \\ C_{7,3}^{(3)} \end{Bmatrix} = \begin{Bmatrix} 0 \\ \tilde{R}_n/24m^4 \end{Bmatrix}. \tag{28, 29}$$

The fact that some constants of the inner solution remain undetermined does not prevent deriving the composite expansion. With respect to the outer solution, the first non-zero solution arises at the fourth order, reading

$$\hat{\Phi}_4 = D_{4,0}^{(1)}e^{\kappa_1\zeta} + D_{4,0}^{(2)}e^{\kappa_2\zeta}. \tag{30}$$

Writing equation (24) for the doublets  $(k, m) = (4, 2)$  and  $(k, m) = (4, 3)$ , and then using equation (29) yields the following solutions for the constants  $D_{4,0}^{(1)}$  and  $D_{4,0}^{(2)}$ :

$$\begin{Bmatrix} D_{4,0}^{(1)} \\ D_{4,0}^{(2)} \end{Bmatrix} = \frac{1}{4m^4} \begin{Bmatrix} 1 \\ \frac{\kappa_1^2(\kappa_1 - \kappa_2)}{-1} \\ -1 \\ \frac{\kappa_2^2(\kappa_1 - \kappa_2)}{\kappa_1^2(\kappa_1 - \kappa_2)} \end{Bmatrix} \tilde{R}_n. \tag{31}$$

A first approximation of the composite expansion can thus be obtained and expressed with the original axial variable  $s$  as follows:

$$\Phi^e = \lambda^4 (D_{4,0}^{(1)}e^{n\kappa_1 s} + D_{4,0}^{(2)}e^{n\kappa_2 s}) + \lambda^7 (C_{7,0}^{(1)}e^{(\rho_1/\beta^{1/4})s} + C_{7,0}^{(2)}e^{(\rho_2/\beta^{1/4})s}). \tag{32}$$

From equations (32) and (3), it is straightforward to derive approximations for the semi-infinite shell mobilities with respect to radial force. For instance, the radial input mobility is given by

$$Y_{wR}^n = \frac{i\omega w|_{s=0}}{R_n} \cong \frac{i\omega \nabla^4 \Phi^e|_{s=0}}{R_n}, \tag{33}$$

which yields the following by retaining the leading term of the respective wave amplitude:

$$Y_{wR}^n = \frac{i\omega\lambda^4}{R_n} \left( (\kappa_1^2 - 1)^2 n^4 D_{4,0}^{(1)} + (\kappa_2^2 - 1)^2 n^4 D_{4,0}^{(2)} - \frac{4m^4\lambda^3}{\beta} (C_{7,0}^{(1)} + C_{7,0}^{(2)}) \right). \tag{34}$$

#### 4. THEORETICAL RESULTS

##### 4.1. DISCUSSION

Approximate expressions for the coefficients of the mobility matrix defined in equation (7) are reported in Tables 1–4. They are lifted from the perturbation analysis conducted with the different components of the excitation. Furthermore, as they are of practical interest in

TABLE 1

Direct mobilities for excitation by axial force ( $n > 0$ );  $\Delta = 1 + (1 - \Omega^2)/n^2$ ,  
 $\sigma^2 = \Omega^2 - [\beta n^2(n^2 - 1)^2/(1 + n^2)]$  and  $\varepsilon_n = \begin{cases} -1 & \text{if } \sigma^2 \leq 0 \\ +1 & \text{if } \sigma^2 \geq 0 \end{cases}$

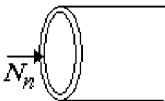
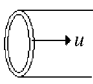
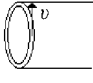
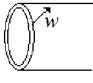
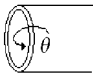
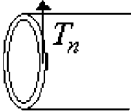
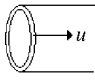
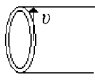
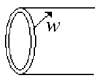
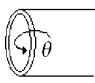
Excitation	Response	Mobility
		$Y_{uN}^n = \frac{\omega R}{n(1 - \mu^2)B} \frac{\varepsilon_n \sqrt{\sqrt{1 - \mu^2} - \sigma} + i\sqrt{\sigma + \sqrt{1 - \mu^2}}}{\sqrt{\sigma}\Delta^{1/4}}$
		$Y_{vN}^n = -\frac{\omega R}{nB(1 - \mu^2)} \frac{\varepsilon_n \sqrt{1 - \mu^2 - \sigma^2} - i\mu\sigma}{\sigma\sqrt{\Delta}}$
		$Y_{wN}^n = \frac{\omega R}{B} \frac{\varepsilon_n}{\sigma\sqrt{\Delta}\sqrt{1 - \mu^2 - \sigma^2}}$
		$Y_{\theta N}^n = -n \frac{\omega}{B} \frac{\varepsilon_n \sqrt{\sqrt{1 - \mu^2} - \sigma} + i\sqrt{\sigma + \sqrt{1 - \mu^2}}}{\sqrt{\sigma}\Delta^{1/4}(1 - \mu^2 - \sigma^2)}$

TABLE 2

Direct mobilities for excitation by circumferential force ( $n > 0$ );  $\Delta = 1 + (1 - \Omega^2)/n^2$ ,  
 $\sigma^2 = \Omega^2 - [\beta n^2(n^2 - 1)^2/(1 + n^2)]$  and  $\varepsilon_n = \begin{cases} -1 & \text{if } \sigma^2 \leq 0 \\ +1 & \text{if } \sigma^2 \geq 0 \end{cases}$

Excitation	Response	Mobility
		$Y_{uT}^n = Y_{vN}^n \text{ (see Table 1)}$
		$Y_{vT}^n = \frac{\omega R}{n(1 - \mu^2)B} \frac{\sqrt{1 - \mu^2 - \sigma^2}(\varepsilon_n \sqrt{\sqrt{1 - \mu^2} + \sigma} - i\sqrt{\sqrt{1 - \mu^2} - \sigma})}{\sigma^{3/2}\Delta^{3/4}}$
		$Y_{wT}^n = -\frac{\omega R}{B} \frac{\varepsilon_n \sqrt{\sqrt{1 - \mu^2} + \sigma} - i\sqrt{\sqrt{1 - \mu^2} - \sigma}}{\Delta^{3/4}\sigma^{3/2}\sqrt{1 - \mu^2 - \sigma^2}}$
		$Y_{\theta T}^n = \frac{n\omega}{B} \frac{\varepsilon_n \sqrt{1 - \mu^2 - \sigma^2} + 2i\sigma}{\sigma\sqrt{\Delta}(1 - \mu^2 - \sigma^2)}$

the field of structure-borne sound, the Green functions associated with the different edge loads derived in the course of the analysis are given in Appendix A. For the sake of brevity, only results concerning the prediction of the radial displacement in the far field are reported.

TABLE 3

Direct mobilities for excitation by radial force ( $n > 0$ );  $\Delta = 1 + (1 - \Omega^2)/n^2$ ,  
 $\sigma^2 = \Omega^2 - [\beta n^2(n^2 - 1)^2/(1 + n^2)]$  and  $\varepsilon_n = \begin{cases} -1 & \text{if } \sigma^2 < 0 \\ +1 & \text{if } \sigma^2 \geq 0 \end{cases}$

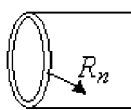
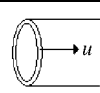
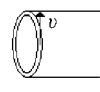
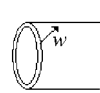
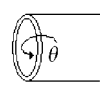
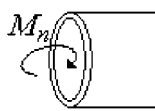
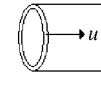
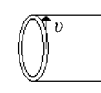
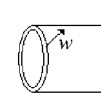

Excitation	Response	Mobility
		$Y_{uR}^n = Y_{wN}^n$ (see Table 1)
		$Y_{vR}^n = Y_{wT}^n$ (see Table 2)
		$Y_{wR}^n = \frac{\omega R}{B} \left( \frac{i\sqrt{2}}{\beta^{1/4}(1 - \mu^2 - \sigma^2)^{3/4}} \right. \\ \left. + n(1 - \mu^2) \frac{\varepsilon_n \sqrt{\sqrt{1 - \mu^2} + \sigma} - i\sqrt{\sqrt{1 - \mu^2} - \sigma}}{\sigma^{3/2} \Delta^{3/4} (1 - \mu^2 - \sigma^2)^{3/2}} \right)$
		$Y_{\theta R}^n = -\frac{\omega}{B} \left( \frac{i}{\sqrt{\beta}\sqrt{1 - \mu^2 - \sigma^2}} + n^2(1 - \mu^2) \frac{2i\sigma + \varepsilon_n \sqrt{1 - \mu^2 - \sigma^2}}{\sigma\sqrt{\Delta}(1 - \mu^2 - \sigma^2)^2} \right)$

TABLE 4

Direct mobilities for excitation by bending moment ( $n > 0$ );  $\Delta = 1 + (1 - \Omega^2)/n^2$ ,  
 $\sigma^2 = \Omega^2 - [\beta n^2(n^2 - 1)^2/(1 + n^2)]$  and  $\varepsilon_n = \begin{cases} -1 & \text{if } \sigma^2 < 0 \\ +1 & \text{if } \sigma^2 \geq 0 \end{cases}$

Excitation	Response	Mobility
		$Y_{uM}^n = Y_{\theta N}^n$ (see Table 1)
		$Y_{vM}^n = Y_{\theta T}^n$ (see Table 2)
		$Y_{wM}^n = Y_{\theta R}^n$ (see Table 3)
		$Y_{\theta M}^n = \frac{\omega}{RB} \left( \frac{i\sqrt{2}}{\beta^{3/4}(1 - \mu^2 - \sigma^2)^{1/4}} \right. \\ \left. + n^3(1 - \mu^2) \frac{\varepsilon_n \sqrt{\sqrt{1 - \mu^2} - \sigma} + i\sqrt{\sqrt{1 - \mu^2} + \sigma}}{\sqrt{\sigma}(1 - \mu^2 - \sigma^2)^2 \Delta^{1/4}} \right)$

Before discussing these results, it is interesting to consider the nature of the free waves associated with the propagation constants given by equation set (20). The two constants  $\rho_i$  appearing in the inner solution occur as a complex conjugate pair when  $\Omega^2 < 1 - \mu^2$ , and thus describe a standing decaying wave (termed wave Type 1 below). Furthermore, the

propagation constants of the outer solution  $\kappa_i$  are also a complex conjugate pair when  $\Omega^2 < \beta n^4$ . Therefore, the vibration field is totally of a nearfield type in this frequency range and all the mobilities are purely imaginary since no propagation of energy is possible. At  $\sigma = 0$  (that is where  $\Omega^2 = \beta n^4$ ), the propagation constants of the outer solution become real and purely imaginary, yielding an evanescent and a propagating wave respectively. They are referred to as Type 2 waves in the rest of this article. The frequency corresponding to  $\Omega^2 = \beta n^4$  is called the cut-on frequency since it indicates the emergence of a propagating wave. This value was obtained by using a simplified set of governing equations, whereas more rigorous shell theories [18] show the cut-on phenomenon occurring at

$$\Omega^2 = \beta n^2 \frac{(n^2 - 1)^2}{1 + n^2}. \quad (35)$$

Consequently, the equation

$$\sigma^2 = \Omega^2 - \beta n^2 \frac{(n^2 - 1)^2}{1 + n^2}, \quad (36)$$

is used instead of equation (10) in the calculation of the mobilities reported in Tables 1–4. For an excitation frequency well above the cut-on frequency of the circumferential mode considered, it appears that the propagation constants of the Type 2 waves tend toward those predicted by the membrane shell theory when tangential inertia is disregarded.

With respect to the very low-frequency behaviour of the beam and the “ovaling” modes ( $n = 1$  and  $2$ , respectively), corrections need to be made to account for the influence of tangential inertial forces. Indeed, within this frequency range, the displacement ratios associated with the Type 2 waves are approximately  $u/w \ll 1$  and  $v/w = -1/n$  [18]. Obviously, inertial force attributed to circumferential vibrations cannot be neglected with regard to this frequency range. Fortunately, this effect can easily be accounted for by applying a correction to the propagation constants  $\kappa_1$  and  $\kappa_2$ . Indeed, by retaining terms arising from the inertial force associated with circumferential motion in the dispersion relation of the membrane theory, it can be shown that the corrected propagation constants can be approximately given by  $\Delta^{1/4}\kappa$  instead of  $\kappa$ , where  $\Delta = 1 + (1 - \Omega^2)/n^2$ . The results reported in Tables 1–4 have thus been obtained by replacing  $\kappa_i$  with  $\Delta^{1/4}\kappa_i$  in the derivation. It can be noted that the approximate expressions confirm the respective importance of the in-plane inertial forces. It is clearly shown from the ratios

$$\frac{\text{Re}(Y_{vX}^n)}{\text{Re}(Y_{wX}^n)} = -\frac{1 - \mu^2 - \sigma^2}{n(1 - \mu^2)} \quad \text{and} \quad \frac{\text{Re}(Y_{uX}^n)}{\text{Re}(Y_{wX}^n)} = \frac{\Delta^{1/4} \sqrt{\sigma} \sqrt{1 - \mu^2 - \sigma^2} \sqrt{\sqrt{1 - \mu^2} - \sigma}}{n(1 - \mu^2)} \quad (37)$$

for a given load component  $X$ , and for frequencies  $\sigma \ll 1$ , that the radial and circumferential displacements generated are of the same order of magnitude when  $n$  is small and much larger than the axial displacement.

From inspecting equation set (20), it appears that the Type 2 wave associated with the propagation constant  $\kappa_1$  remains evanescent regardless of the frequency. In fact, when axial inertial force is considered, it can be shown that this wave becomes propagating at [18]

$$\Omega^2 = (1 - \mu)n^2/2. \quad (38)$$

Accordingly, this wave only propagates in the  $n = 1$  mode below the ring frequency. The influence of this change in character manifests itself in the real part of the mobilities by a high axial input mobility, small peaks of amplitude for  $Y_{\theta M}^n$  and  $Y_{uM}^n$  and local dips in the frequency curves for the remaining mobilities. However, since axial inertial force was not considered in the formulation of the problem, these patterns will not be reflected by the approximated solutions.

Tables 1–4 reflect the membrane-type behaviour of the shell for frequencies well above the cut-on frequency of the mode but below the ring frequency. Indeed, the existence of the Type 1 wave shows itself only in the imaginary part of the mobilities  $Y_{wR}^n$ ,  $Y_{\theta R}^n$  and  $Y_{\theta M}^n$ , thereby resulting in a high compliance of the shell with respect to out-of-plane excitation. The vibrational power that is proportional to the real part of the mobilities is thus governed by the Type 2 waves and proportional to  $\beta^{-1/2}$ . The strong coupling between the different shell displacements is reflected by the fact that the cross-mobilities are of the same order of magnitude as the input mobilities. This coupling is also evidenced by the equations (A2–A5) provided in Appendix A, where the radial displacement in the far field is of the same order of magnitude, whatever the load type exerted on the shell. Finally, as regards the dependence of input mobilities upon  $n$ , it can be seen in Tables 1–4 that the circumferential modes become either harder or softer with respect to in-plane and out-of-plane excitations, respectively, as their order  $n$  increases.

#### 4.2. EXCITATION OF SHELLS BY RADIAL FORCE

Of considerable interest is the asymptotic expression of  $Y_{wR}^n$  at very low frequency ( $\Omega^2 \ll 1$ ). In this frequency range, the contribution of the Type 1 wave can be neglected and the input radial mobility reads

$$Y_{wR}^n = \frac{n\omega R}{B(1 - \mu^2)^{1/4}} \frac{\epsilon_n - i}{(\Omega^2 - \beta n^2(n^2 - 1)^2/(1 + n^2)^{3/4}(1 + 1/n^2)^{3/4})} \quad \text{for } \Omega^2 \ll 1. \quad (39)$$

For the beam mode ( $n = 1$ ), upon assuming that a total force of 1 N is applied on the shell in such a manner that only the  $n = 1$  mode is excited, the distribution of radial force is then given by  $R_n = 1/\pi R$  and the velocity at the excitation point is

$$\dot{w} = Y_{wR}^n R_n = \frac{\omega(1 - i)}{B(1 - \mu^2)^{1/4} \Omega^{3/2} 2^{3/4} \pi} = \frac{1 - i}{\rho S c_B}, \quad (40)$$

where  $c_B = \sqrt{\omega^4 EI/\rho S}$ ,  $S$  is the area of the shell cross-section ( $S = 2\pi R h$ ) and  $I$  its moment of inertia ( $I = \pi h R^3$ ). It can be seen that this corresponds to the mobility of a semi-infinite Euler beam excited at its end [10]. For modes  $n \geq 2$ , the radial displacement due to a force distribution given by  $R_n = 1 \text{ N/m}$  is

$$w = \frac{n(1 - \mu^2)^{3/4}}{\beta^{5/4} E \sqrt{6(n^2 - 1)^{3/2}}}, \quad \text{when } \Omega^2 \ll \beta n^2 \frac{(n^2 - 1)^2}{1 + n^2}, \quad (41)$$

which is the result obtained by Simmonds [7] in the static case when  $2 \leq n \leq ((1 - \mu^2)/4\beta)^{1/4}$ .

Another point of significant interest is the comparison of these results to those for infinite shells. In Appendix B, the problem of the infinite shell excited in its “middle” by a radial

force distribution is formulated according to the matched asymptotic expansions method. However, as the mathematical procedure is very similar, only the expression derived for the radial input mobility is presented, being

$$Y_{wR}^{n,\infty} = \frac{\omega R}{4B} \left( \frac{i\sqrt{2}}{\beta^{1/4}(1-\mu^2-\sigma^2)^{3/4}} + n\sqrt{1-\mu^2} \frac{\varepsilon_n(\sqrt{1-\mu^2}+\sigma)^{3/2} - i(\sqrt{1-\mu^2}-\sigma)^{3/2}}{\sigma^{3/2}\Delta^{3/4}(1-\mu^2-\sigma^2)^{3/2}} \right) \quad (42)$$

and where

$$\varepsilon_n = \begin{cases} -1 & \text{if } \sigma^2 < 0, \\ +1 & \text{if } \sigma^2 \geq 0. \end{cases} \quad (43)$$

Upon assuming  $\Omega \ll 1$ , equation (42) reduces to the formula provided by Heckl [3]. Furthermore, from Table 3 and equation (42), it can be shown that the ratio of the real parts of the mobilities for the infinite and semi-infinite shells is given by

$$\frac{\text{Re}(Y_{wR}^{n,\infty})}{\text{Re}(Y_{wR}^{n,\infty/2})} = \frac{1}{4} \left( 1 + \frac{\sqrt{\Omega^2 - \beta n^4}}{\sqrt{1-\mu^2}} \right) \quad \text{where } \beta n^4 < \Omega^2 < 1 - \mu^2 \quad (44)$$

and the superscripts  $\infty$  and  $\infty/2$  refer to the infinite and the semi-infinite shell respectively. The ratio given by equation (44) is independent of the circumferential modal number  $n$  and tends towards  $1/4$  at very low frequencies, which is the same as in the beam case [10].

Finally, the case of radial excitation lends itself to a study of the result's validity. From the expression for  $Y_{wR}^n$  given in Table 3, it can be seen that infinite responses of the shell are predicted at frequencies given by  $\sigma = 0$  and  $\sigma^2 = 1 - \mu^2$ . The former is the lower cut-on frequency of the mode while the latter corresponds to a singularity introduced by the perturbation method. In fact, results obtained numerically do indeed show a higher shell response in the vicinity of  $\sigma^2 = 1 - \mu^2$  for the lower circumferential modes, but the peak of magnitude remains finite; with its amplitude decreasing rapidly as the order  $n$  increases. It is worth noting that this type of non-uniformity is related to out-of-plane motions only and does not appear in the mobility expressions for the in-plane displacements  $u$  and  $v$ . It can be shown that the non-uniformity region around  $\sigma^2 = 1 - \mu^2$ , where the approximate solutions cease to be valid, grows proportionally to the factor  $\sqrt{\beta n^2}$ . Removing this singularity can be achieved by introducing a detuning parameter in a manner similar to the one described in reference [9]. Once this is done, an approximate expression for the real part of the input radial mobility can be derived for frequencies contained in the range  $\beta n^4 < \Omega^2 \leq 1 - \mu^2$ , reading

$$\text{Re}(Y_{wR}^n) = \frac{\omega R}{B} n(1-\mu^2) \frac{\sqrt{\sqrt{1-\mu^2}+\sigma}}{\sigma^{3/2}\Delta^{3/4}((1-\mu^2-\sigma^2)^{3/2} + 2\sqrt{\beta n^2\sigma^2})}, \quad (45)$$

which yields the following at  $\Omega = \sqrt{1-\mu^2}$ :

$$\text{Re}(Y_{wR}^n) = \frac{\omega R}{nB\sqrt{2\beta(1-\mu^2)}}. \quad (46)$$

5. COMPARISON WITH NUMERICAL RESULTS

In this section, the accuracy of the approximate solutions is shown by comparing mobilities calculated by using the approximate solutions given by Tables 1–4 to numerical results obtained by using Flügge theory [14, 16]. The parameters of the shell used for the comparison are described in Table 5.

Consider a load type  $X$  applied at the edge of the semi-infinite shell and the resulting velocity  $\dot{\alpha}$  at a point in the shell section  $x = 0$ .  $X$  symbolizes the excitation components  $N_s$ ,  $T_s$ ,  $R_s$  and  $M_s$ , and  $\dot{\alpha}$  symbolize one of the velocities  $\dot{u}$ ,  $\dot{v}$ ,  $\dot{w}$  and  $\dot{\theta}$ , and are assumed to have Fourier series expansions of the form

$$X(x = 0, \phi) = \sum_{n=0}^{\infty} X_n \cos\left(n\phi - \frac{\pi}{2} \delta_{XT}\right) + \sum_{n=0}^{\infty} \underline{X}_n \sin\left(n\phi - \frac{\pi}{2} \delta_{XT}\right) \quad \text{and} \quad (47)$$

$$\dot{\alpha}(x = 0, \phi) = \sum_{n=0}^{\infty} \dot{\alpha}_n \cos\left(n\phi - \frac{\pi}{2} \delta_{\alpha v}\right) + \sum_{n=0}^{\infty} \underline{\dot{\alpha}}_n \sin\left(n\phi - \frac{\pi}{2} \delta_{\alpha v}\right), \quad (48)$$

where

$$\delta_{XT} = \begin{cases} 0 & \text{if } X \neq T \\ 1 & \text{if } X = T \end{cases} \quad \text{and} \quad \delta_{\alpha v} = \begin{cases} 0 & \text{if } \dot{\alpha} \neq \dot{v} \\ 1 & \text{if } \dot{\alpha} = \dot{v} \end{cases}$$

In these expansions, the first sum is associated with the loads ( $N_s$ ,  $T_s$ ,  $R_s$ ,  $M_s$ ) and the solutions ( $\dot{u}$ ,  $\dot{v}$ ,  $\dot{w}$ ,  $\dot{\theta}$ ) having a dependence upon the azimuthal co-ordinate  $\phi$  of the form  $(\cos(n\phi), \sin(n\phi), \cos(n\phi), \cos(n\phi))$  while the underlined terms are of the form  $(\sin(n\phi), \cos(n\phi), \sin(n\phi), \sin(n\phi))$ . In the problem formulation, the first kind of solution was assumed, yielding the mobility matrix  $[Y_{ij}^n]$  as defined in equation (7). By a similar reasoning, a matrix  $[\underline{Y}_{ij}^n]$  can also be defined for the Fourier components  $\underline{\dot{\alpha}}_n$  and  $\underline{X}_n$ . However, the form adopted in equations (46) and (47), ensures the equality  $[\underline{Y}_{ij}^n] = [Y_{ij}^n]$ , and from equations (48) and (7), it follows that

$$\dot{\alpha}(0, \phi) = \sum_{n=0}^{\infty} Y_{\alpha X}^n X_n \cos\left(n\phi - \frac{\pi}{2} \delta_{\alpha v}\right) + \sum_{n=0}^{\infty} Y_{\alpha X}^n \underline{X}_n \sin\left(n\phi - \frac{\pi}{2} \delta_{\alpha v}\right). \quad (49)$$

The errors introduced by using the approximate solutions given in Tables 1–4 for the assessment of the real part of the input mobilities have been estimated in decibels. Figure 2 shows contour plots of the error in the  $\Omega$ - $n$  plane for  $Y_{uN}^n$ ,  $Y_{vT}^n$ ,  $Y_{wR}^n$  and  $Y_{\theta M}^n$  (isoline at 1.5 dB). The curves corresponding to the cut-on frequencies given by equations (35) and (38) are also shown. As it can be shown that the errors are approximately proportional to  $\beta^{1/4}n$  or to  $\beta^{1/2}n^2$ , these curves can then be extrapolated to any shell by

TABLE 5

*Physical properties of the shell*

Density, $\rho$ (kg/m <sup>3</sup> )	7800
Young's modulus, $E$ (N/m <sup>2</sup> )	$2.1 \times 10^{11}$
Poisson ratio, $\mu$	0.3
Radius, $R$ (m)	0.5
Thickness-to-radius ratio, $h/R$	0.02

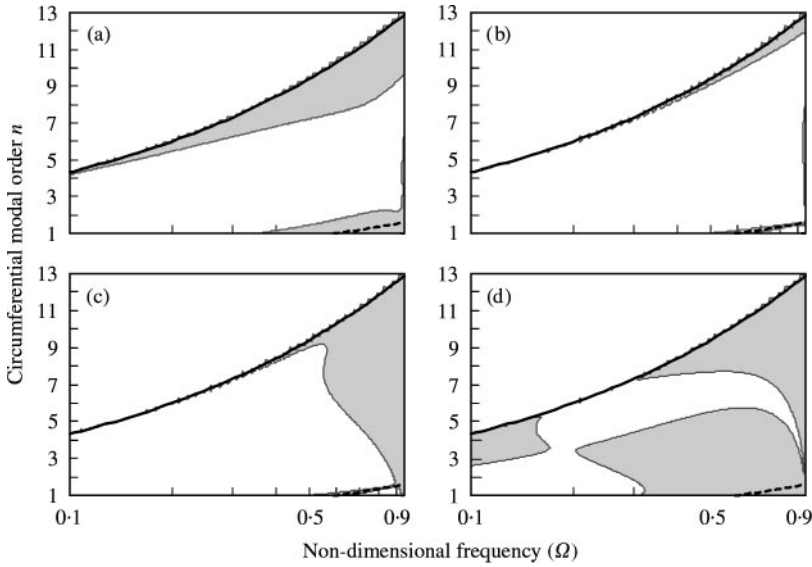


Figure 2. Contour plots of the error in  $Y_{\alpha X}^n$  in decibels in the  $\Omega$ - $n$  plan: (a)  $Y_{uN}^n$ ; (b)  $Y_{vT}^n$ ; (c)  $Y_{wR}^n$ ; (d)  $Y_{\theta M}^n$ ; (white region) = error < 1.5 dB, (grey region) = error > 1.5 dB, —, equation (35); - - -, equation (38).

keeping the  $\beta^{1/4}n$  product constant. However, in the case at hand, it must be realized that the plots given in Figure 2, though represented as continuous functions of  $n$ , have a physical significance for integer values of  $n$  only. Figure 2 shows that the error increases proportionally to the circumferential order but is higher closer to the cut-on frequencies. Furthermore, the non-uniformity regions for  $Y_{wR}^n$  and  $Y_{\theta M}^n$  around the singularity at  $\sigma^2 = 1 - \mu^2$  are seen to grow larger as  $n$  increases. Figure 2(c) shows poorer agreement for  $Y_{\theta M}^n$ , even for modes of low circumferential order  $n$ . This can be attributed to the fact that the following term in the expansion of the real part of  $Y_{\theta M}^n$  is only an order of  $\beta^{1/4}n$  lower than the leading term, while for the other mobilities, there is a difference in the order of  $\beta^{1/2}n^2$ .

The approximate solutions were also used to estimate the shell response to point excitations applied at  $x = 0, \phi = 0$ . For point load, the Fourier components of the load  $X$  are given by

$$\begin{cases} X_n = \frac{X}{2\pi R} \tau_n \\ \underline{X}_n = 0 \end{cases} \text{ for } X = N_s, R_s \text{ or } M_s \quad \text{and} \quad \begin{cases} X_n = 0 \\ \underline{X}_n = -\frac{X}{2\pi R} \tau_n \end{cases} \text{ for } X = T_s, \quad (50)$$

where

$$\begin{cases} \tau_n = 1 & \text{when } n = 0, \\ \tau_n = 2 & \text{when } n > 0. \end{cases}$$

The direct mobilities are easily obtained by inserting equation (50) into equation (49):

$$Y_{\alpha X} = \frac{\dot{\alpha}(s = 0, \phi = 0)}{X} = \begin{cases} 0 & \text{if } \dot{\alpha} = \dot{v} \text{ and } X \neq T \text{ or } \dot{\alpha} \neq \dot{v} \text{ and } X = T, \\ \frac{1}{2\pi R} \sum_{n=0}^{\infty} \tau_n Y_{\alpha X}^n & \text{otherwise.} \end{cases} \quad (51)$$



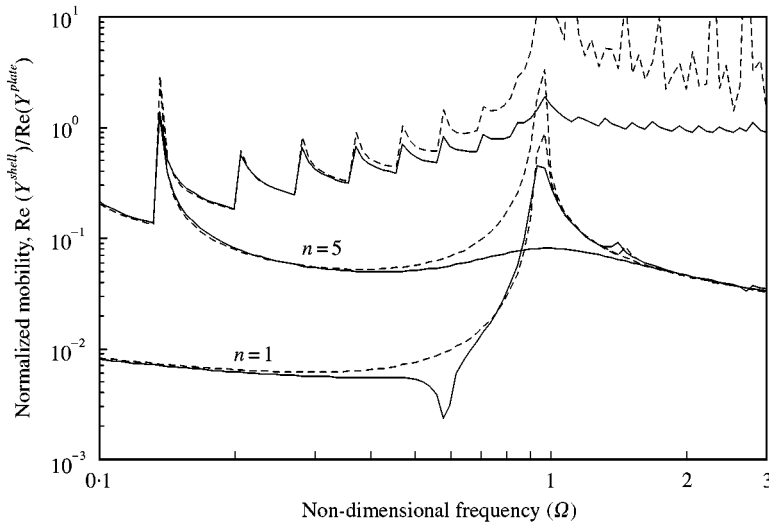


Figure 3. Real part of the input radial mobility for the cylindrical shell normalized by the semi-infinite plate one and contributions of different circumferential modes. —, Flügge theory; ----, approximate solutions.

By way of illustration, Figure 3 shows the real part of the input radial mobility plotted against non-dimensional frequency and obtained by using both Flügge theory and the approximate solution for  $Y_{wR}^n$  given in Table 3. The mobility is normalized by the corresponding mobility for a semi-infinite plate,  $Y^{plate} = 0.462/\sqrt{\rho h D}$  [19]. The contributions of the circumferential modes  $n = 1$  and  $5$  to the total mobility are also shown. As expected, the semi-infinite plate mobility is a good approximation of the frequency-averaged mobility of the semi-infinite shell when  $\Omega > 1$ . The maxima exhibited by the mobility correspond to the cut-on frequencies given by equation (40) while the beam mode ( $n = 1$ ) exhibits a dip at the cut-on frequency given by equation (38). Finally, comparing approximate and numerical results shows acceptable agreement in the frequency region  $\Omega < 0.5$ , and the non-uniformity at  $\sigma^2 = 1 - \mu^2$  clearly appears responsible for the increasing discrepancy as the frequency approaches the ring frequency.

Figure 4 shows the real parts of the direct mobilities defined in equation (51) plotted against non-dimensional frequency for the cylindrical shell described by Table 5. Equation (45) is used instead of the expression given in Table 3 for the input radial mobility. For the axisymmetric mode ( $n = 0$ ), the approximate solutions derived in reference [9] were used together with the input circumferential mobility

$$Y_{vT}^0 = \frac{\omega R}{B} \frac{\sqrt{2}}{\Omega \sqrt{(1 - \mu)(1 + 3\beta)}}. \quad (52)$$

Figure 4 shows that the approximate solution yields acceptable agreement for  $\Omega < 0.5$ . Above this frequency, agreement for the axial input mobility is strongly affected by the influence of inertial force in the axial direction of the  $n = 1$  mode and for mobilities related to out-of-plane motions by the non-uniformity at  $\sigma^2 = 1 - \mu^2$ . Upon comparing Figures 3 and 4(c), it appears that the accuracy of the approximate solution is greatly improved when the singularity is removed as in equation (45).

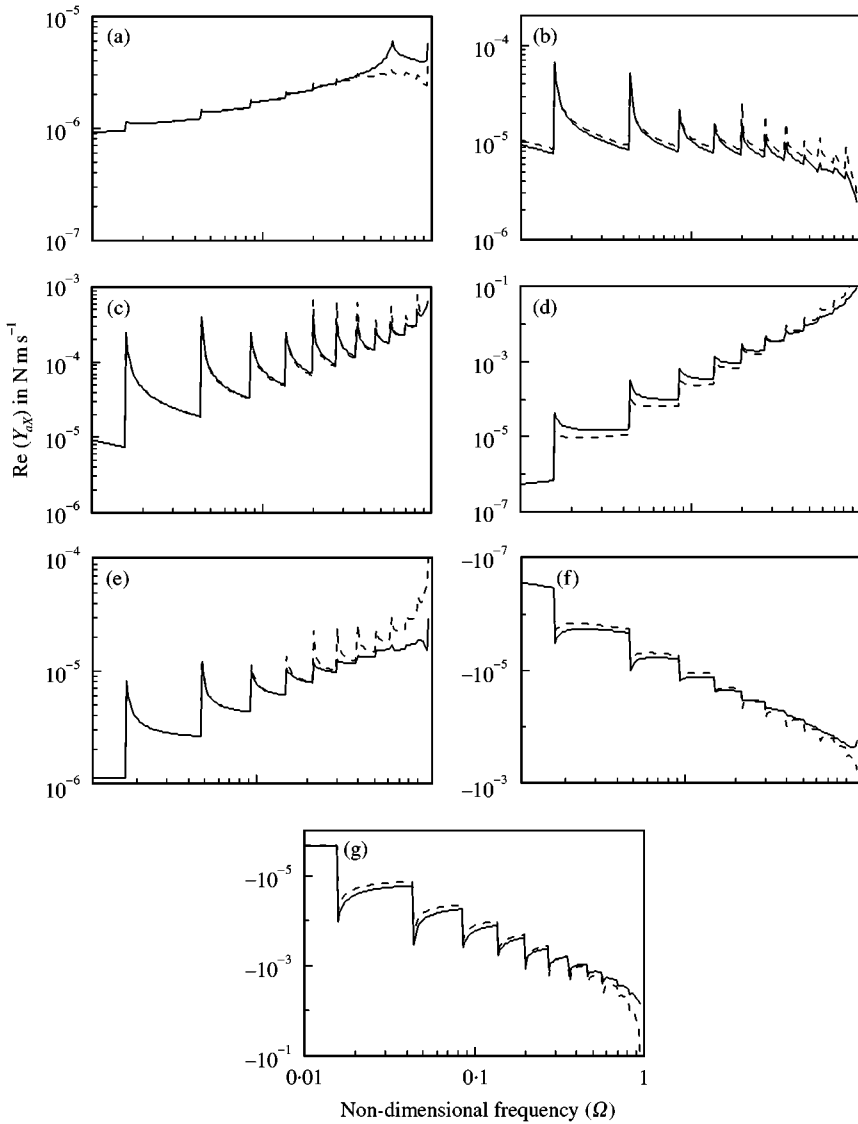


Figure 4. The real part of the point mobilities: (a)  $Y_{uN}^n$ ; (b)  $Y_{vT}^n$ ; (c)  $Y_{wR}^n$ ; (d)  $Y_{\theta M}^n$ ; (e)  $Y_{wN}^n$ ; (f)  $Y_{\theta N}^n$  and (g)  $Y_{\theta R}^n$ : —, Flüge theory; ----, Tables 1-4.

## 6. CONCLUSION

A perturbation technique has been applied to study the dynamic response of a semi-infinite, thin-walled shell to forces and moment applied at its edge. Considering a given circumferential mode of low order only ( $n = 1, 2, 3 \dots$ ), approximate closed-form solutions have thus been derived for the associated input and cross-mobilities. The perturbation analysis allows the bending effects localized in the edge region to be accounted for, while bringing to the fore the membrane behaviour of the shell for these modes of vibration. Solutions are obtained in the form of power-series expansions, with the expansion parameter being a function of both the mode order  $n$ , and the shell thickness

parameter. The analytical expressions derived display the functional dependence of the solutions on the problem parameters, revealing the strong coupling taking place between the in-plane and out-of plane motions of the shell below the ring frequency. Furthermore, owing to the waveguide behaviour of the shell, the expressions derived enable the prediction of the vibrational power transmission by point excitation. Finally, the accuracy of the expressions derived has been discussed in terms of both the individual modal mobilities and the point mobilities, showing that acceptable agreement is obtained for frequency below half the ring frequency.

#### ACKNOWLEDGMENTS

The author would like to gratefully acknowledge the support for this work provided by the Swedish National Energy Administration, along with Professors S. Ljunggren and J.-L. Guyader, and Dr S. Finnveden for their valuable discussions.

#### REFERENCES

1. X. M. ZHANG and R. G. WHITE 1993 *Structural Intensity and Vibrational Energy Flow—4th International Congress on Intensity Techniques, Senlis, France, August 31–September 2*. Vibrational power input to a cylindrical shell due to point force excitation.
2. P. A. FRANKEN 1960 *Journal of the Acoustical Society of America* **3**, 473–477. Input impedances of simple cylindrical structures.
3. M. HECKL 1962 *Journal of the Acoustical Society of America* **34**, 1553–1557. Vibration of point-driven cylindrical shells.
4. C. R. FULLER 1983 *Journal of Sound and Vibration* **87**, 409–427. The input mobility of an infinite circular cylindrical elastic shell filled with fluid.
5. G. V. BORGIOTTI and E. M. ROSEN 1992 *Journal of the Acoustical Society of America* **91**, 911–925. The state vector approach to the wave and power flow analysis of the forced vibrations of a cylindrical shell. Part I: Infinite cylinders in vacuum.
6. S. FINNVEDEN 1997 *Journal of Sound and Vibration* **208**, 705–728. Formulas for modal density and for input power from mechanical and fluid point sources in fluid filled pipes.
7. J. G. SIMMONDS 1966 *Journal of Mathematics and Physics* **45**, 127–149. Influence coefficients for semi-infinite and infinite circular cylindrical shells.
8. R. S. MING, J. PAN and M. P. NORTON 1999 *Journal of the Acoustical Society of America* **105**, 1702–1713. The mobility functions and their application in calculating power flow in coupled cylindrical shells.
9. O. FÉGEANT 2001 *Journal of Sound and Vibration* **243**, 89–115. Closed-form solutions for the point mobilities of axisymmetrically excited cylindrical shells.
10. L. CREMER, M. HECKL and E. E. UNGAR 1973 *Structure-borne Sound*. Berlin: Springer-Verlag.
11. J. D. KAPLUNOV 2000 *Journal of the Acoustical Society of America* **107**, 1383–1393. Free localized vibrations of a semi-infinite cylindrical shell.
12. K. GRAFF 1975 *Wave Motion in Elastic Solids*. Oxford: Clarendon Press.
13. S. K. WONG and W. B. BUSH 1993 *Journal of Sound and Vibration* **160**, 523–531. Axisymmetric vibrations of a clamped shell using matched asymptotic expansions.
14. W. FLÜGGE 1973 *Stresses in Shells*. Berlin: Springer-Verlag.
15. W. SOEDEL 1993 *Vibration of Shells and Plates*. New York: Marcel Dekker; second edition.
16. A. W. LEISSA 1973 *Vibrations of Shells* (NASA SO-288). Washington, D.C.: U.S. Government Printing Office.
17. A. H. NAYFEH 1973 *Perturbation Methods*. New York: John Wiley & Sons, Inc.
18. P. W. SMITH 1955 *Journal of the Acoustical Society of America* **27**, 1065–1072. Phase velocities and displacement characteristics of free waves in a thin cylindrical shell.
19. C. KAUFFMANN 1998 *Journal of the Acoustical Society of America* **103**, 1874–1884. Input mobilities and power flows for edge-excited, semi-infinite plates.

## APPENDIX A: GREEN FUNCTIONS FOR THE SEMI-INFINITE SHELL

Being a stage in the derivation of the mobilities, Green functions for the semi-infinite shell excited at the edge are reported here when farfield conditions are met, that is at a distance from the edge where the decaying standing wave and the evanescent wave can be disregarded in the expression of the solution.

In the frequency range  $\beta n^4 \ll \Omega^2 \ll 1 - \mu^2$ , the farfield criterion can be defined as

$$\frac{n\sqrt{\Omega}x}{R} \gg 1 \quad (\text{A1})$$

and Green functions from axial force, tangential force, radial force and bending moment to the radial displacement  $w_n$  read as follows, respectively,

$$G_{wN}^n(x|0) = -\frac{R}{2B\sqrt{1-\mu^2}} \frac{1}{\sigma\sqrt{\Delta}} \left( 1 + i\sqrt{\frac{\sqrt{1-\mu^2}+\sigma}{\sqrt{1-\mu^2}-\sigma}} \right) e^{n\Delta^{1/4}\kappa_2 x/R}, \quad (\text{A2})$$

$$G_{wT}^n(x|0) = \frac{R}{2B\sqrt{1-\mu^2}} \frac{\sqrt{\sqrt{1-\mu^2}+\sigma}}{\sigma^{3/2}\Delta^{3/4}} \left( 1 + i\sqrt{\frac{\sqrt{1-\mu^2}+\sigma}{\sqrt{1-\mu^2}-\sigma}} \right) e^{n\Delta^{1/4}\kappa_2 x/R}, \quad (\text{A3})$$

$$G_{wR}^n(x|0) = -\frac{nR\sqrt{1-\mu^2}}{2B} \frac{\sqrt{\sqrt{1-\mu^2}+\sigma}}{\sigma^{3/2}\Delta^{3/4}(1-\mu^2-\sigma^2)} \left( 1 + i\sqrt{\frac{\sqrt{1-\mu^2}+\sigma}{\sqrt{1-\mu^2}-\sigma}} \right) e^{n\Delta^{1/4}\kappa_2 x/R}, \quad (\text{A4})$$

$$G_{wM}^n(x|0) = \frac{n^2\sqrt{1-\mu^2}}{2B} \frac{1}{\sigma\sqrt{\Delta}(1-\mu^2-\sigma^2)} \left( 1 + i\sqrt{\frac{\sqrt{1-\mu^2}+\sigma}{\sqrt{1-\mu^2}-\sigma}} \right) e^{n\Delta^{1/4}\kappa_2 x/R}, \quad (\text{A5})$$

where

$$\Delta = 1 + \frac{1-\Omega^2}{n^2}, \quad \sigma^2 = \Omega^2 - \frac{\beta n^2(n^2-1)^2}{1+n^2} \quad \text{and} \quad \kappa_2 = -i\sqrt{\frac{\sigma}{\sqrt{1-\mu^2}-\sigma}}.$$

## APPENDIX B: INPUT RADIAL MOBILITY OF THE INFINITE CYLINDRICAL SHELL

Consider a shell of infinite extent vibrating in its  $n$ th circumferential mode as a result of a radial force distribution  $R_n$  applied in its “middle”. This problem can be transformed into a boundary-value problem by considering a semi-infinite shell and the following set of boundary conditions,

$$u_n|_{s=0} = 0, \quad v_n|_{s=0} = 0, \quad w_n|_{s=0} = 0, \quad \frac{R_n}{2} = \frac{D}{R^3} (w_n'' + (2-\mu)w_n''')|_{s=0}, \quad (\text{B1})$$

which are in accord with the symmetry of the infinite shell. By using equation (3), equations (B1) can then be expressed in terms of the function  $\Phi_n$ . Upon adopting the form of the solution given by equation (11), and the inner axial variable  $\zeta$ , the boundary conditions

associated with the inner solutions are given by

$$\begin{aligned} \tilde{\Phi}'_k = 0, \quad \tilde{\Phi}''_k + \frac{1}{\mu} \tilde{\Phi}'_{k-2} = 0, \quad \tilde{\Phi}'''_k - \frac{1}{2 + \mu} \tilde{\Phi}'_{k-2} = 0, \\ \tilde{\Phi}''''''_k - (4 - \mu) \tilde{\Phi}''''_{k-2} + (5 - 2\mu) \tilde{\Phi}''_{k-4} - (2 - \mu) \tilde{\Phi}'_{k-6} = \frac{\tilde{R}_n}{2} \delta_{k7}. \end{aligned} \quad (\text{B2})$$

The matching conditions and the form of the composite solution are unaffected by the change of boundary conditions from equations (14) to (B2). By following a similar reasoning as the one adopted in section 3.4, an approximate solution is finally obtained for the input radial mobility, being

$$Y_{wR}^n = \frac{\omega R}{4B} \left( \frac{i\sqrt{2}}{\beta^{1/4}(1 - \mu^2 - \sigma^2)^{3/4}} + n\sqrt{1 - \mu^2} \frac{\varepsilon_n(\sqrt{1 - \mu^2} + \sigma)^{3/2} - i(\sqrt{1 - \mu^2} - \sigma)^{3/2}}{\sigma^{3/2} \Delta^{3/4} (1 - \mu^2 - \sigma^2)^{3/2}} \right). \quad (\text{B3})$$